J Polym Environ (2016) 24:287–297
DOI 10.1007/s10924-016-0771-x

ORIGINAL PAPER

Reactive Compatibilization of Biobased Polyurethane Prepolymer Toughening Polylactide Prepared by Melt Blending

Thangavel Gurunathan[1,2] · Jin Suk Chung[1] · Sanjay K. Nayak[2]

Published online: 25 July 2016

Abstract Polylactide (PLA) is a major biodegradable polymer, which has received extensive interests over the past decades and holds great potential to replace several petroleum-based polymeric materials. Nevertheless, the inherent brittleness and low impact strength have restricted its invasion to niche markets. In this paper, the authors demonstrate that the entirely bio-sourced blends, namely PLA and castor oil-based polyurethane prepolymer (COPUP), were first melt-compounded in an effort to prepare novel biodegradable materials with an excellent balance of properties. NCO-terminated COPUP was successfully synthesized and subsequently mixed with variable concentration of PLA matrix using melt-compounded by twin-screw extrusion technique. The miscibility, phase morphology, mechanical properties, and thermal resistance of the blends were investigated. During FTIR analysis, it suggests that the interfacial compatibilization between COPUP and PLA phase occurred by the reaction of –NCO group of MDI with terminal hydroxyl group of PLA. DMA analysis showed that COPUP and PLA showed some limited miscibility with shifted glass transition temperature. The morphologies of fracture surface showed a brittle-to-ductile transition owing by the addition of COPUP. The crystallization behavior was studied by differential scanning calorimeter (DSC). The strain at break and notched impact strength of PLA/COPUP blends were increased more than 112–15.4 times elegant of neat PLA; the increase is superior to previous toughening effect by using petroleum-based tougheners. Furthermore, the thermal resistances and melt flow properties of the materials were also examined by analysis of the melt flow index and heat deflection temperature use in the work. With enhanced toughness, the PLA/COPUP blends could be used as replacements for some traditional petroleum-based polymeric materials.

Keywords Polylactide · Toughening · Castor oil-based polyurethane prepolymer · Mechanical properties

Introduction

Plant-derived polylactide (PLA; $(–CHCH_3–CO–O–)_n$) is the most extensively investigated and much attracted due to the sustainability and environmental concerns with respect to the traditional petroleum-based polymers [1]. It has a number of excellent properties including biocompatibility, biodegradability, good mechanical properties and easy processability [2, 3]. PLA offers great promise in a wide range of commodity applications and competes with poly(ethylene terephthalate) (PET) and polystyrene (PS) for many automotive industries, biomedical materials, and food packaging applications [4–6]. However, the brittleness of PLA about its relatively low values of tensile strain at break, tensile toughness and impact strength (2 J m^{-1} for notched specimens of PLA) have imposed constraints for many applications [7]. Therefore, numerous studies have been carried out to overcome the brittleness of PLA in the past few years, and the solutions proposed include the addition of rigid fillers [8], copolymerizations [9], plasticization [10], and blending with flexible polymers [11–14]. Among various approaches, reactive blending provides an

✉ Thangavel Gurunathan
juru001@gmail.com

[1] School of Chemical Engineering, University of Ulsan, Namgu, Daehakro 93, Ulsan 680-749, Republic of Korea

[2] Central Institute of Plastics Engineering and Technology, Guindy, Chennai 600032, India

economic and effective way to modify the properties of PLA. For instance, various biobased and petroleum-based ductile polymers have been employed to blend with PLA to improve its toughness, including bacterially produced poly(hydroxyalkanoate) (PHA) [14], polyamide elastomer (PAE) [15], poly(ethylene oxide) (PEO) [16], poly(ε-caprolactone) (PCL) [12], poly(butylene succinate) (PBS) [17], poly(butylene adipate-co-terephthalate) (PBAT) [18], polymerized and conjugated soybean oil (PSO, CSO) [19, 20], hyperbranched poly(ester-amide) [21], bacterial polyesters [22], ethylene-co-vinyl acetate (EVA) [23], acrylonitrile–butadiene–styrene copolymer (ABS) [24], TEMPO-oxidized cellulose [25], crosslinked polyurethane [26], poly(vinyl alcohol) (PVA) [27], poly(oxymethylene) (POM) [28], and starch [29]. Unfortunately, most of those blends are immiscible with PLA and thus could not remarkably improve the flexibility of the end materials; Hence to obtain a high toughness of PLA blends, compatibilization is essential. The compatibility of blends can be improved by adding suitable block or graft copolymers [9]. However, most of the above blends yielded very limited enhancement in impact strength, especially in the notched situation [7].

In recent years, reactive blending represents a more effective way to prepare high- performance polymer blends which has been newly introduced to modify their properties by changing the molecular structure of the polymer or to improve the compatibility of blends [11]. However, limited work has been carried out to modify PLA by reactive blending in an earlier studies. Recently, Oyama [11] reported super-tough PLA blends with poly(ethylene-glycidyl methacrylate) (EGMA) (80/20, w/w) prepared by reactive blending, which showed an impact strength superior to benchmark acrylonitrile–butadiene–styrene (ABS) resins. Harada et al. [30] investigated the blends of PLA/PBS using L-lysine-triisocyanate (LTI) as a reactive processing agent, and the results suggested that the blends have better impact strength and tensile strain than those of neat PLA.

Polyurethane (PU) is an ideal choice for toughening PLA as it has a combination of toughness, elasticity and high strength, as well as biocompatibility and biodegradability [31, 32]. In addition, the soft segments of plant oil-based PU prepolymer mainly polyester or polyether is expected to have an excellent compatibility with PLA because PLA has been reported to be miscible with some polyesters or polyethers [16]. Also, the possibility of hydrogen bonding between the carbamate (R–O–CO–NH_2) group of plant oil-based polyurethane prepolymer (PUP) and the carbonyl (C=O) groups of PLA support the assumption of potential miscibility and good compatibility with the matrix polymer [33]. Li et al. [31] have shown that adding TPU elastomer to PLA can gradually transform brittle to ductile fracture. They were able to increase notched impact strength over five times by adding 30 wt% TPU. In this study, renewable resources-based castor oil (CO) is used as a polyol. This polyol can be used as a precursor for the synthesis of polyurethane because of its hydroxyl functionality, and relatively inexpensive plant oil obtained from the seed of *Ricinus Communis* [34, 35]. The triglyceride of CO is derived from ricinoleic acid (12-hydroxy-9-octadecenoic acid), which constitutes of 90 % of fatty acids present in the molecule and 10 % non-hydroxylated fatty acids, mainly oleic and linoleic acids. Due to this particular chemical composition, CO becomes highly valuable for polyurethane chemistry [34].

Earlier we explored the studies on melt-blended PLA with COPUP at various compositions and found improvement in properties for samples containing 30 wt% COPUP [36]. With 30 % of COPUP, strain at break went from 3.5 to 359 % and notched Izod impact strength improved from 24.98 to 269.62 J m^{-1}. However, instead of blending, the mechanical property can be further improved without an obvious drop in the tensile strength. To the best of our knowledge there are no reports about the binary blends of PLA and COPUP has been investigated so far. Therefore, our complete intention is to produce blends of PLA and COPUP with increased toughness while maintaining biostability. To gain biodegradable blends with the appropriate melt strength, stiffness-toughness the balance along with requisite thermal performance. The specific objectives of this research are to assess the miscibility, crystallization behavior; phase morphology, mechanical properties, and thermal resistance of the binary system were investigated.

Experimental Section

Materials

PLA (4042D), a semi-crystalline extrusion grade, was supplied by NatureWorks LLC (USA), with M_w = 110,000 - g/mol, M_w/M_n = 2.1, L-lactide and D-lactide ratio 92:8, density 1.24 g/cm^3, melt flow index (MFI) between 1 and 2 g/10 min (190 °C, 2.19 kg, ASTM D1238) was taken as the base matrix. PLA was dried overnight at 80 °C prior to use in a desiccating dryer. Castor oil (local suppliers), with characteristic properties of hydroxyl value (OHV) (156–165 mg/KOH g^{-1})and an acid value (AV) (1.27–3 mg/KOH g^{-1}) measured according to ASTM standards D 1639-89 and D 4274-94, respectively. The methylene diphenyl diisocyanate (MDI), dibutylamine, and dibutyltin dilaurate (DBTDL) were purchased from Aldrich (Milwaukee, WI, USA). Methyl ethyl ketone (MEK) was purchased from Fisher Scientific Company (Mumbai, India). All other chemicals of analytical grade were used without further purification.

Experimental Techniques

Synthesis of the NCO-Terminated Castor Oil-Based Polyurethane (PU) Prepolymer

The synthesis of NCO-terminated castor oil-based polyurethane (PU) prepolymer was carried out in two-step reaction sequence. The castor oil was dried in a vacuum for 6 h at 70 °C in an oil bath before being used. In the first step, the castor oil reacted with an excess of MDI were placed into a four-necked round-bottomed flask assembled with a mechanical stirrer, reflux condenser, heating mantle, dropping funnel and nitrogen flushing. The reaction was maintained at 75–80 °C for nearly 2–3 h in the presence of 1 wt% of DBTDL as a catalyst. During the synthesis, samples were extracted each 30 min in triplicate and diluted in methyl ethyl ketone and mixed with 20 mL of a standard solution of dibutylamine 0.05 molar in toluene for the reaction between the residual diisocyanate and the amine, to control the NCO consumption during the reaction. The excess amine was titrated against 1.0 N HCL, using bromophenol blue as indicator. For each titration, 25 mL of isopropyl alcohol was added to the solution to ensure compatibility between dibutylamine and the HCL solution. The reaction ratio of NCO/OH was calculated from 56.1 % of NCO groups were consumed at the end of the prepolymer synthesis. The final prepolymer cured in an oven at 60 °C for 2 days. The reaction ratio of –NCO/–OH was calculated using the process reported by Gurunathan et al. [36].

Preparation of the PLA/Castor Oil-Based PUP Blends

The prepolymer was further melt-blended in a second step by reactive processing with the adequate amount of PLA. The prepolymer synthesized in the first step and the calculated amount of PLA were directly introduced in the feeding zone of an internal mixer (M/s DSM, Xplore 15 mL, Netherlands) equipped with mini injection molder. The mixing was carried out at a screw speed of 100 rpm and with a temperature profile of 170, 175, 180 °C for the three successive zones and total cycle time was around 10 min. Finally, specimens were prepared using mini injection molding machine at a mould temperature of 30 °C, injection time of 5 s, injection pressure of 7–8 bar and melt temperature of 170 °C as per ASTM standards to analyze the mechanical properties.

Characterizations

IR Spectroscopy

The FTIR of the samples was done using Thermo Scientific Nicolet^{TM} 6700 spectrometer in attenuated total reflection infrared (ATR) mode, within the frequency range of 4000–400 cm^{-1} by co-adding 32 scans and at a resolution of 4 cm^{-1} with strong apodization.

Differential Scanning Calorimetry (DSC)

Differential scanning calorimetry was performed on a thermal analyzer (DSC, Q20, M/s TA Instruments, USA). Sample of ~3 mg were heated at a rate of 10 °C/min from 25 to 200 °C to remove the thermal history, equilibrated at −50 °C and then heated to 200 °C to determine glass transition (T_g), cold crystallization (T_{cc}), melting (T_m) and heat of fusion (ΔH_m). The whole process was carried out under the protection of nitrogen flow of 20 mL/min.

Dynamic Mechanical Analysis (DMA)

Dynamic mechanical properties were measured using a dynamic mechanical analyzer (DMA, Q800, M/s TA Instruments, USA) operated in multifrequency strain mode, using a single cantilever clamp, following the standard ASTM D4065. All samples were trimmed to 63.5 × 12.7 × 3 mm^3 were performed at a temperature range from −100 to 100 °C at a heating rate of 5 °C/min, strain of frequency 1 Hz, and amplitude 15 μm were used during testing. Liquid nitrogen was used to regulate temperature during heating and cooling.

Scanning Electron Microscopy (SEM)

The morphologies of blends were investigated by scanning electron microscopy (SEM; Zeiss EVO-MA, UK) instrument at an accelerating voltage of 10 kV. All of the samples were frozen in liquid nitrogen (about 15 min) and fractured. The fractured surfaces were sputter-coated with a thin layer of gold prior to examination.

Transmission Electron Microscopy (TEM)

The morphology of the dispersed phase was performed by transmission electron microscopy (JEM 1400 TEM mode, JEOL, Japan) at an accelerated voltage of 100 kV. The ultrathin sections (60–80 nm in thickness) were cryogenically sliced at −80 to −100 °C using a Cryo Leica EM UC6 instrument (Leica Microsystems, Switzerland) with a diamond knife and viewed without staining.

Mechanical Properties

Tensile properties, including tensile strength, tensile modulus and strain at break, were determined in accordance with the ASTM D638 using specimens of dimensions 165 × 13 × 3 mm were strained at a crosshead speed of

5 mm/min and gauge length of 50 mm in Universal testing machine, (UTM, Instron 3386 UK).

For Izod impact tests the sample of dimension 63.5 × 10 × 3 mm, were notched at angle of 45° with a V notch depth of 2.54 mm were used. Subsequently, the measurements were carried out in an Impactometer (6545, M/s Ceast, Italy) as per ASTM-D-256. The testing was carried out at standard laboratory conditions of 23 ± 5 °C + 55-/.RH. A minimum of five replicate specimens was tested for each material, and the data reported are from the average of five.

Heat Deflection Temperature (HDT) and Melt Flow Index (MFI)

The heat deflection temperature (HDT) of neat PLA and blends were determined with an HDT tester (Toyoseiki Co., Japan) according to the ASTM D648 using dimensions of the test bars 127 mm × 13 mm × 3 mm. The loading pressure was 0.455 MPa (66 psi) and the samples were heated at a rate of 2 °C min^{-1} from ambient temperature to the desired temperature in a three-point bending mode. The HDT was reported as the temperature at which the deflection of 0.25 mm occurred.

Melt flow index (MFI) of the PLA/COPUP was tested according to ASTM D1238 at 190 °C with a load of 2.16 kg by using a Melt Flow Indexer (Qualitest model 2000A). Material was first pelletized before analysis. Melt index was calculated as follows:

$$MI = \frac{W \times 600}{t}$$

where MI is melt index, g/10 min; W is the average weight of the spline, g; t is the sampling interval, s.

Results and Discussion

Reactive Interfacial Compatibilization

Figure 1 demonstrates the FTIR spectra of CO, neat PLA, COPUP, and PLA/COPUP blends. The broad peak of the hydroxyl group (–OH) appears at 3445–3500 cm^{-1} for CO and neat PLA. The peak intensities of the end groups consistently appear quite weak because of their low molar content in the respective polymeric chains. The FTIR spectra are mainly characterized by broad and medium intensity peak around 3350 cm^{-1} arises which shows the stretching vibration of –NH bond in the urethane segments (–NHCOO–). The absorption bands as observed at 2840–2946 cm^{-1} due to –CH stretching vibrations: asymmetric $–CH_3$ stretching at 2942 cm^{-1}, asymmetric $–CH_2$ stretching at 2944 cm^{-1}, symmetric $–CH_3$ stretching at

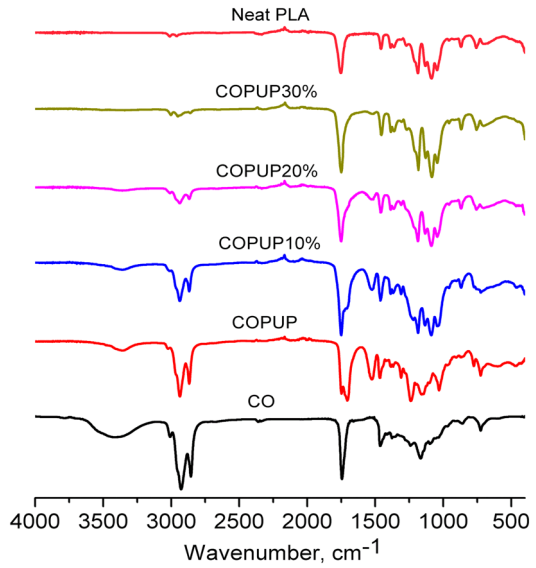

Fig. 1 FTIR spectra of CO, neat COPUP, PLA and PLA/COPUP blends

2837 cm^{-1} and symmetric $–CH_2$ stretching at 2868 cm^{-1} [4]. The N=C=O peaks in MDI at 2270 cm^{-1} appeared and disappeared, clearly implying the successful preparation of COPUP. The amide-I mode is a highly complex vibration and involves the contribution of the –C=O stretching, the –CN stretching and the –C–C–N deformation vibrations. The complexity and multiplicity of inter- or intramolecular environments surrounding the carbonyl groups in polymers make the amide-I range considerably broader in polymers that occur in the region of 1600–1800 cm^{-1} [37]. In the present study, the band is observed corresponding to 1762, 1756 and 1753 cm^{-1}, respectively, for COPUP, COPUP10 %, COPUP20 %, and COPUP30 % polymers.

The peak at 1522, 1526 and 1528 cm^{-1} (amide II, $\delta_{N–H} + \nu_{C–N} + \nu_{C–C}$; sensitive to chain conformation and intermolecular hydrogen bonding) [36], 1310–1350 cm^{-1} (amide III, $\delta_{N–H} + \nu_{C–N}$). The amide IV, V, and VI bands are produced by highly mixed modes containing a significant contribution from the –NH out-of-plane deformation mode, expected to be in the 800–400 cm^{-1} [38]. A feeble single band as observed at 868 cm^{-1}, which might be originating from the coupled vibration of either the C–O stretching or CH_2 rocking modes. All these spectral changes provide convincing evidence for the formation of urethane-urea functionality.

The hydroxyl (–OH) stretching band of PLA, if subjected to intermolecular hydrogen bonding or any other chemical interaction, may provide evidence of compatibility or partial compatibility. The neat PLA shows a band centered at 3504 cm^{-1} in the –OH stretching region and can be attributed to the end carboxyl group of the PLA. When the PLA is mixed with the COPUP to form blends,

the peak at 3504 cm^{-1} disappears, indicating the occurrence of chemical interaction between the end carboxyl and hydroxyl groups of the PLA and –NH groups of the COPUP. The absorption at 1758 cm^{-1} is assigned to the carbonyl (–C=O) stretching vibration of the PLA [39, 40]. In the PLA/COPUP blends, upon increasing COPUP content, the intensity of the peak decreases and another peak at 1725 cm^{-1} assigned to the ν(C=O) absorbance of the grafted COPUP disappears. This indicates that, with increasing COPUP content, more and more carbonyl groups of the COPUP are involved in PLA-rich phase and interact with those of the PLA.

Thermal Behavior of the PLA/COPUP Blends

The physical, mechanical, and thermal resistance properties of these polymers greatly depend on the solid-state morphology and its crystallinity. Consequently, it is paramount to study the influence of the existence of the COPUP on the crystallization of PLA. Figure 2 shows the DSC second-heating curves of neat PLA and the blends after melt-quenched, with a heating rate of 10 °C min^{-1}. From the scans, three transitions could be found, namely PLA glass transition, an exothermic cold-crystallization peak, and a melting endothermic peak. As expected, the glass transition temperature (T_g) of PLA and COPUP in the blends shifted toward lower temperature because of reactive blending, but the change observed was very little. The T_g of COPUP in the reactive blend found to be at −22.6, −23.3, −23.9 and −24.8 °C, respectively, for PLA/COPUP5 %, PLA/COPUP10 %, PLA/COPUP20 % and PLA/COPUP30 %. The value of T_g gradually decreased with increasing COPUP content, implying that the blends showed some limited miscibility. It was consistent with the results from DMA and SEM analysis.

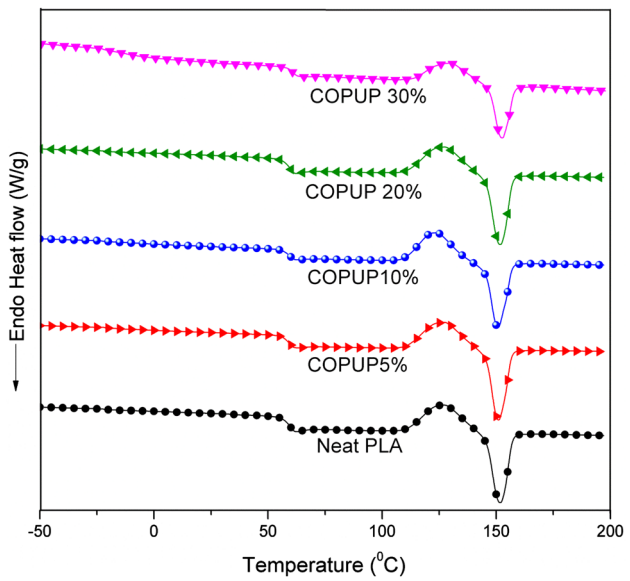

Fig. 2 DSC second heating curves of the neat PLA and PLA/COPUP blends with a heating rate of 10 °C/min

The cold crystallization peak temperature (T_{cc}) of neat PLA is around 126.7 °C. The cold crystallization of the PLA in the blend is accelerated after extension of the COPUP as evidenced by a reduction in T_{cc} (by 4 °C) with broad cold-crystallization peaks. The COPUP is carrying out broadening of the peak of T_{cc} rather than altering the T_{cc} with increasing in concentration. So, it is evident that COPUP is acting like chain extender and modifying the T_{cc} temperature range. The reason for this enhancement of cold-crystallization of PLA by the addition of COPUP can be attributed to the following reason. As discussed in previous results, COPUP show limited miscibility with PLA, and there was sufficient chain mobility locally activated, the cold-crystallization will be improved due to the easily dynamic chain alignment. During the second heating scan, the unmelted COPUP domains might act as a nucleating center and thereby enhance the crystallization of the PLA in blends, which was observed in the PLA/PES and PLA/PCL blend system [41, 42]. Recently, Hong et al. [43] thoroughly studied the nucleation enhancement effect in the PLA/TPU blend, which was a system with some limited miscibility. The author pointed out that the phase interface seems to play an F role in the nucleation enhancement effect in the blends. In addition, neat PLA shows a melting peak at 153.3 °C. All of the samples showed only one T_m, which was consistent with that of neat PLA, indicating that the introduction of COPUP did not influence much on the crystal structure of PLA.

Table 1 shows the heat of cold-crystallization (ΔH_{cc}) and the heat of melting (ΔH_m) decreased continuously upon increasing COPUP content in the blends, suggesting that the degree of crystallinity of the PLA component was hardly changed regardless of the content of COPUP. The results can be attributed to molecular interactions between the PLA and the COPUP, which has been demonstrated by the shifted T_g obtained by DMA. The similar events were also obtained in other immiscible PLA blends such as PLA/PBAT and PLA/PCL [7, 44].

Thermo-Mechanical Properties

Dynamic mechanical analysis (DMA) was used to study the effect of composition of COPUP on the compatibility of PLA/COPUP blends. Figure 3a, b shows the storage modulus and tan delta as a function of temperature for neat PLA and PLA/COPUP blends with different COPUP content. Glass transition temperature of the polymer blend is critically important to evaluate the miscibility of the components [45–47]. Two distinct peaks can be

Table 1 Thermal properties of neat PLA and PLA/COPUP blends

Sample	$T_{g,COPUP}$[a] (°C)	$T_{g,COPUP}$[b] (°C)	$T_{g,PLA}$[a] (°C)	$T_{g,PLA}$[b] (°C)	T_{cc} (°C)	T_m (°C)	ΔH_{cc} (J/g)	ΔH_m (J/g)
Neat PLA			61.9	71.9	126.7	153.3	22.3	24.1
COPUP5 %	−22.6	−36.8	59.6	70.2	124.8	153.7	20.6	23.0
COPUP10 %	−23.3	−42.2	58.7	69.8	123.7	153.4	20.4	21.3
COPUP20 %	−23.9	−47.4	58.4	69.6	122.5	153.7	17.8	20.1
COPUP30 %	−24.8	−55.8	57.1	67.8	120.1	154.9	15.9	17.2

[a] Determined by DSC measurement, [b] determined by DMA measurement

observed on the tan delta plots. The glass transition temperature (T_g) were calculated from the tan delta peak temperature and are summarized in Table 1. As observed in Fig. 3a tan δ curves, pristine polymer showed one peak (glass transition) and all of the blends demonstrated two distinct glass transitions, revealing a typical two-phase system, one for COPUP at about −36.8 to −55.8 °C and one for PLA at about 71.9 to 67.8 °C, indicating that the blends are thermodynamically miscible. However, the T_g of both COPUP and PLA shifted 3–9 °C inwards towards each other when the composition ratios were varied, suggesting that COPUP and PLA were partially miscible and that there are some degree of macromolecular affinity between the two components. In the case of COPUP molecule, the castor oil as the soft segment (polyether) and diisocyanate (IPDI) as a hard segment (polyamide). The soft segment played an important role of enhancing the compatibility between the PLA and COPUP through melt-compounding. The hard segment of COPUP can make an interaction with the PLA molecules theoretically. The hard segment containing amide groups can form hydrogen bonds with the PLA molecules. As it is well-known, the hydrogen bond can enhance interfacial adhesion and improve better compatibility. PLA has indeed been reported to be miscible with some polyethers, such as PPG and PEO [6].

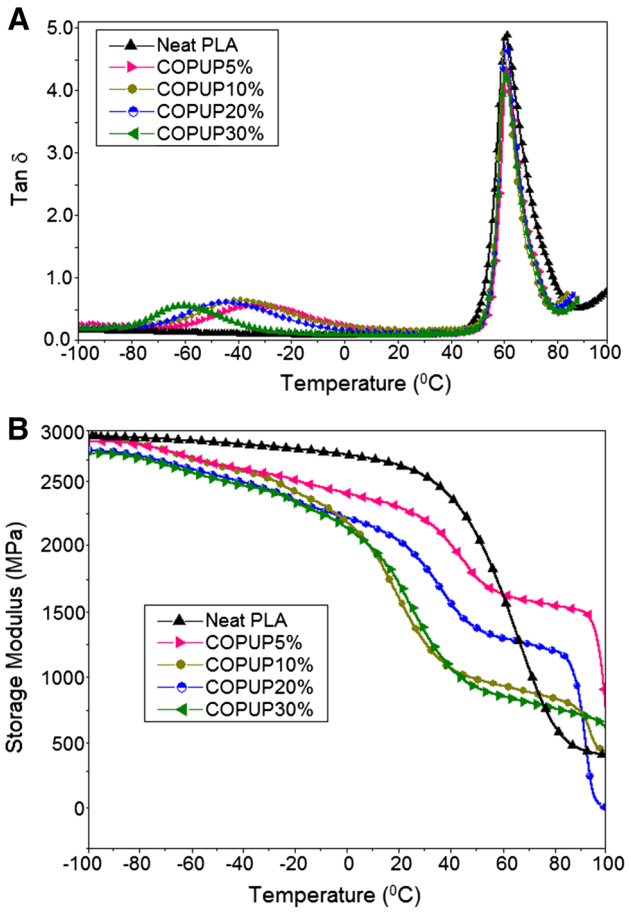

Fig. 3 Dynamic viscoelastic curves of neat PLA and its blends: **a** tan δ versus temperature; **b** storage modulus versus temperature

As shown in Fig. 3b, the storage modulus (E') at room temperature for PLA/COPUP blends gradually decreased with increasing content of COPUP. The E′ of the PLA and its blends dropped significantly around 45–65 °C due to the glass transition of PLA and lack of crystallinity. However, as the temperature increased, the storage modulus dropped rapidly, so there was not much appreciable improvement in the tensile test that were performed at room temperature. These phenomena are in agreement with the above DSC results.

Phase Morphology of the PLA/COPUP Blends

It is a well known factor that, phase behavior plays a vital role in mechanical behavior of polymer blends. The types of morphology and the size of dispersed phases in the polymer blends are important factors that determine physical properties and rheological behavior [48]. Therefore, both SEM and TEM were applied to characterize the phase morphology of multiphase blends. Figure 4 presents the SEM micrographs for the cryofractured surface of neat PLA and PLA/COPUP blends with different COPUP contents. Neat PLA showed a smooth surface for different regions without visible elastic deformation in the stress

direction, suggesting brittle fracture corresponding to the low impact strength. The impact fractured surfaces of PLA/COPUP blends showed a remarkable difference from that of neat PLA. PLA/COPUP showed much rougher surface with more fibrils on fracture surface, suggesting the occurrence of extensive plastic deformation through shear yielding of the PLA matrix. The castor oil-based PU prepolymer act as stress concentrators because they have an elastic property that differed from the PLA matrix. The formation of such surface would receive more impact energy through rubber stretching and tearing COPUP and PLA; thus show greater impact strength and toughness [49], which was consistent with the results obtained by DMA measurements where two glass transitions were obtained corresponding to the two phases, as discussed in "Phase Morphology of the PLA/COPUP Blends" section. There was no break between the two phases, and the phase boundary was obscure, implying that there was adequate interfacial adhesion between the two phases. The above results imply that the content of COPUP plays a crucial role in the mechanical properties of the PLA blends.

The TEM analysis was further applied to identify the morphological structure of PLA/COPUP blends. Cryomicrotome gaunt samples were undertaken TEM investigation. From Fig. 5, showing TEM observation, it was clearly evident that PLA/COPUP blends well-dispersed droplet-in-matrix structure. PLA/COPUP presented more homogeneous phase morphology with smaller COPUP dispersed particle size. The size of the ion increased progressively with the COPUP content proportional to blend composition, which is in good agreement with results obtained by SEM analysis.

Effect of COPUP Content on the Mechanical Properties of the PLA/COPUP Blends

In general, the mechanical properties of a polymer can be roughly classified into two categories: toughness and strength. The Izod impact strength and tensile elongation are considered as the material toughness, whereas the tensile strength and flexural modulus are the material strength [50]. The tensile strength, elongation at break, and Young's modulus of neat PLA and PLA/COPUP blends were obtained by a tensile test. Figure 6 shows the tensile stress–strain curves of neat PLA and the blends and Table 2 summarizes the details of the tensile properties. Neat PLA is very rigid and brittle with tensile strength around 61.1 MPa, tensile modulus of 2601.20 MPa, and elongation at break only about 3.56 %. There was no yield observed in the case of neat PLA, which presented a high-tensile strength and destitute toughness. On the contrary, the addition of COPUP significantly changed the tensile behavior of the PLA as

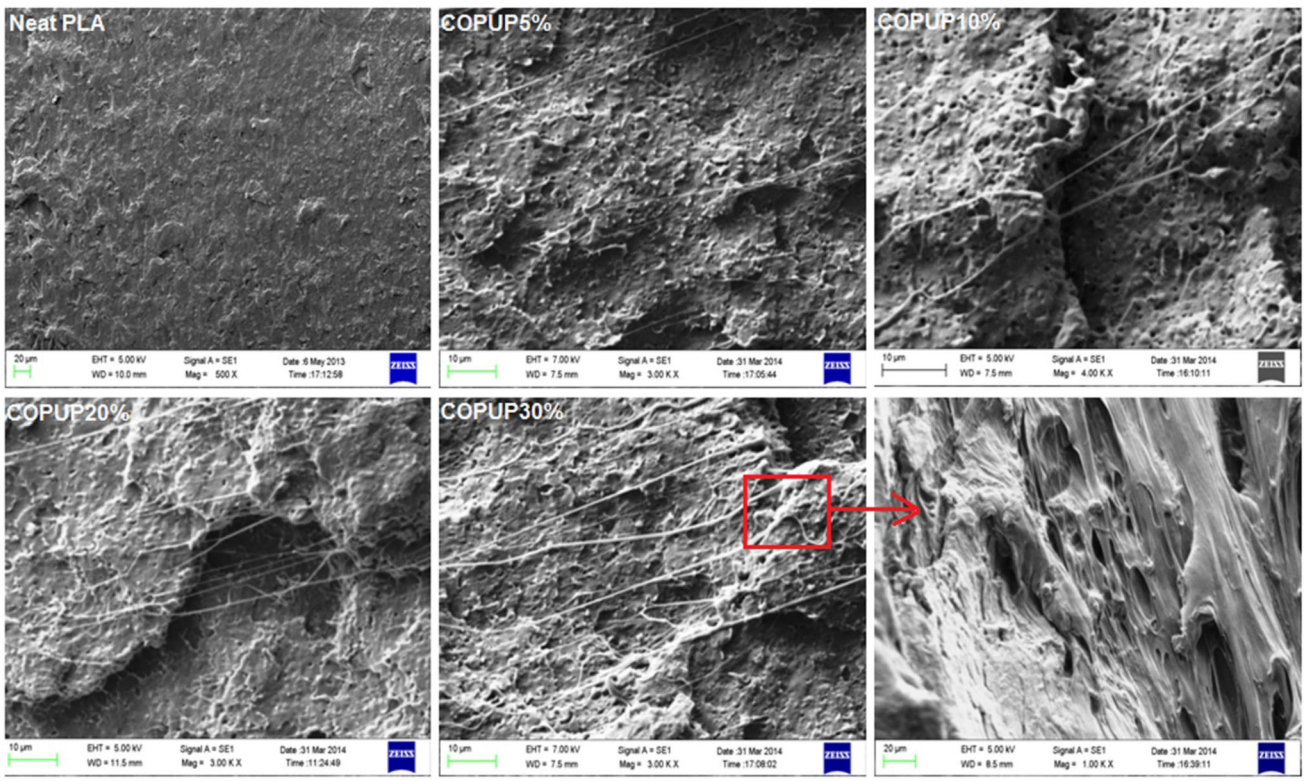

Fig. 4 SEM micrographs of impact fracture surface of neat PLA and its blends

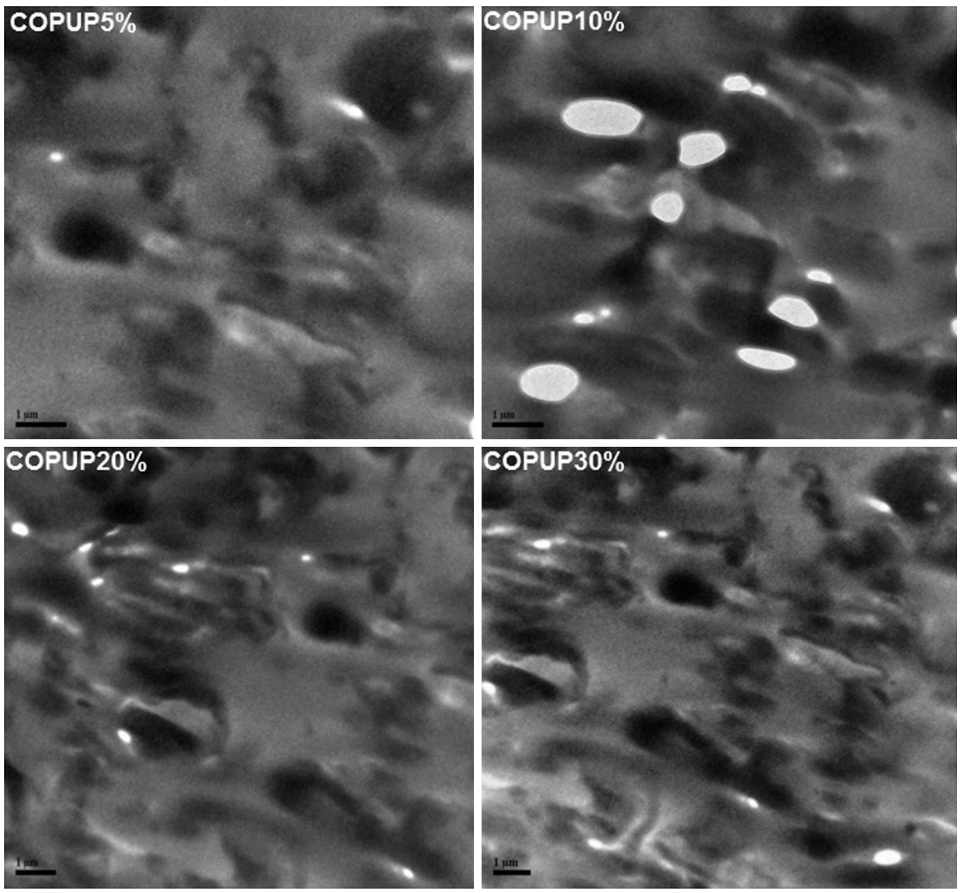

Fig. 5 TEM micrograph of PLA blends with different COPUP content

shown in Fig. 7, and all of the blends show typical yielding behavior and stable neck growth. This result indicates that the brittle fracture of the neat PLA transformed into ductile fracture of the PLA/COPUP blends, upon them being subjected to tensile testing. It is notable that the elongation at break of PLA is improved consistently with the addition of 10 % COPUP, and a remarkable increase was obtained when the COPUP content was further increased to 30 %. Conversely, the tensile strength of the blends more decreased with increasing COPUP content in a nearly linear manner (about 10 % lower). When the weight fraction of COPUP reached 30 %, the PLA/COPUP blends showed an optimum increase in percentage elongation to the tune of 401.3 %, which was higher than those of PLA/TPU [43], PLA/PBS/DCP [17], PLA/Poly(ether)urethane elastomer [31], PLA/PBS/clay [51], and PLA/PBSL blends [52]. On the other hand, the tensile strength and Young's modulus decreased not too much compared with neat PLA, being 61.19 (neat PLA) to 33.1 MPa (COPUP30 %) and 2601.2 (neat PLA) to 1477.3 MPa (COPUP30 %). The significant improvement of stain at the break of the blend suggests some degree of molecular interaction between the diisocyanate (–NCO) hard segments (COPUP) and polyester macroglycol (–OH) soft segments (PLA) and dipole–dipole or intermolecular hydrogen bonding formed between the molecules of the blended matrix [43, 53].

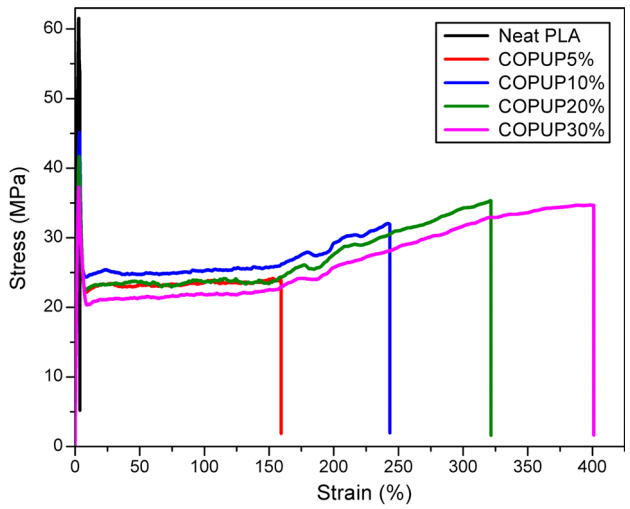

Fig. 6 Tensile stress–strain curves of neat PLA and its blends

The Izod impact strength evaluation is an important tool to study the COPUP on the impact toughness to PLA blends. Figure 8 also compares the impact strength of neat PLA with that of the blends at room temperature, and the

Table 2 Mechanical properties, HDT and MFI of neat PLA and PLA/COPUP blends

Composition	UTS (MPa)	YS (MPa)	*E* (MPa)	ε_b (%)	IS (J m^{-1})	HDT (°C)	MFI (190 °C) g/10 min
Neat PLA	61.19 ± 5.1	55.9 ± 2.4	2601.2 ± 71.4	3.56 ± 0.80	24.9 ± 3.4	55.2 ± 0.5	32.2 ± 1.1
COPUP5 %	56.9 ± 3.9	54.2 ± 1.0	1996.5 ± 29.3	160.2 ± 13.4	101.5 ± 16.4	59.3 ± 0.3	34.7 ± 1.8
COPUP10 %	47.7 ± 2.6	44.6 ± 3.9	1876.1 ± 48.2	243.5 ± 18.3	196.3 ± 23.1	62.5 ± 0.6	35.3 ± 2.0
COPUP20 %	38.5 ± 2.8	36.2 ± 1.5	1692.4 ± 62.3	322.8 ± 28.1	297.1 ± 41.2	71.8 ± 0.3	37.1 ± 2.7
COPUP30 %	33.1 ± 1.0	30.3 ± 1.7	1477.3 ± 32.8	401.3 ± 33.1	384.7 ± 35.2	75.1 ± 0.8	39.6 ± 3.8

UTS Ultimate tensile strength, *YS* yield stress, *E* Young's modulus, ε_b strain at break, *HDT* heat deflection temperature, *MFI* melt flow index

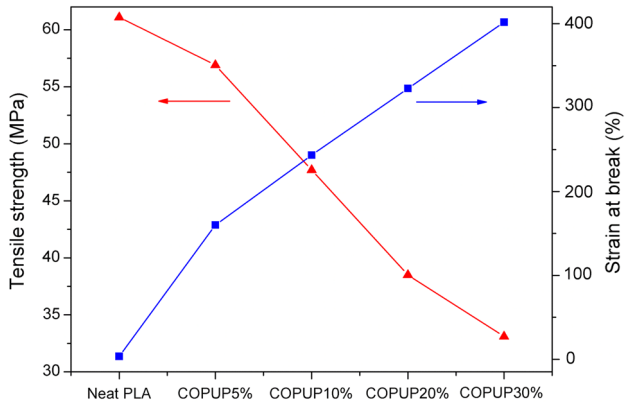

Fig. 7 Tensile strength and the elongation at break with different COPUP concentrations

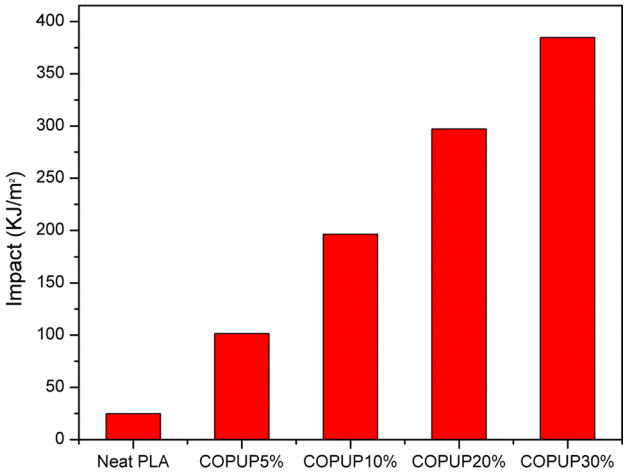

Fig. 8 Effect of COPUP concentrations in the blends on their impact strength

results are shown in Table 2. Neat PLA showed impact strength of only 24.9 J m^{-1}, indicating the samples clearly fractured in a brittle manner. The impact strength of PLA/COPUP10 % was 196.3 J m^{-1} which was about 7.8 times that of neat PLA. Significant improvement can be observed for blends PLA/COPUP30 %, which was approximately 15.4 times higher than that of neat PLA. It is well-known that toughness implies energy absorption and can be achieved through addition of a second flexible phase in the form of particles [54]. It could be observed that the toughness of the samples steadily increased with the increasing content of COPUP, which was consistent with the variation tendency in the tensile strain of the samples.

HDT and MFI Determination

The HDT denotes the upper working temperature limit of the plastic and is described as the temperature at which the material will deflect 0.25 mm under load of 0.455 MPa [55]. In order to determine the thermal resistance under practical applications, the HDT of the PLA/COPUP blends were determined according to the ASTM D 648 as shown in Table 2. The neat PLA and COPUP have the HDT of 55.2 and 136 °C, respectively, which is reasonable as explained by Hashima et al. [56] that the HDT of an amorphous polymer is around its glass transition temperature, and that of a highly crystalline polymer is at the proximity of its melting point. For the PLA/COPUP blends, there was a significant improvement in HDT from 55.2 °C for neat PLA to 75.1 °C for 30 wt% PLA/COPUP blend. It seems that the HDT of PLA governs the overall thermal resistance of the binary blends with PLA as matrix. The significant temperature increment here may be due to an increase in crystallization ability of PLA in the blends. When the content of COPUP increased, the HDT increased to a higher temperature.

The melt flow index measurement was an important method to characterize the processing properties of polymer melt. The results of the MFI measurements are represented in Table 2. The MFI of neat PLA shows above 32.2 g/10 min whereas high viscosity is observed for neat COPUP with a value at 13.9 g/10 min. It can be observed that the MFI of the blends is increased sharply even though a small amount of COPUP is included, which indicates that adding COPUP dramatically improves the plasticization of the blends and modifies the melt viscosity. The MFI results

show that the blends show more excellent flow behavior compared to the neat polymer, which are beneficial for the filler or filler-reinforced composites uses.

Conclusions

The present work highlights the efficiency of the CO that could be successfully utilized for the synthesis of NCO-terminated polyurethane prepolymers. For the first time in the literature, these NCO-terminated COPUP were used as host materials for melt blending PLA to get renewable resources based on PLA/COPUP blends. The interfacial compatibilization occurred between COPUP and PLA by reaction of -NCO group of MDI with the terminal hydroxyl groups of the PLA matrix. The strain at break and notched impact strength of the blends of PLA were improved dramatically through the formation of PLA/COPUP binary blends in which COPUP dispersed well in the PLA matrix. The failure mode changed from brittle fracture of the neat PLA to ductile fracture of the blends, as demonstrated by the SEM micrographs of impact-fracture surface. The DMA analysis observed that PLA/COPUP blends are a partially miscible system because of the hydrogen bonding between the molecules of COPUP and PLA. DSC results showed that the addition of COPUP, not only accelerates the crystallization rate of PLA, but also reduces the PLA crystallinity. The stress–strain curves of the PLA blends exhibit an elastic deformation that takes place in the PLA matrix. The thermal resistance of PLA was improved by the addition of COPUP. Based on the mechanical and HDT results, the PLA/COPUP blend shows an effective strategy with good balanced stiffness-toughness and thermal resistance. Our research indicates that these biobased PLA/COPUP blends can hopefully be used as substitutes for traditional petroleum-based polymers such as polypropylene and polyethylene.

Acknowledgments The authors are thankful to Department of Chemicals and Petrochemicals (DCPC), Ministry of Chemicals and Fertilizers, Government of India (GOI) for sponsoring the Project.

References

1. Liu HZ, Zhang JW (2011) J Polym Sci B Polym Phys 49:1051–1083
2. Kale G, Kijchavengkul T, Auras R, Rubino M, Selke SE, Singh SP (2007) Macromol Biosci 7:255–277
3. Wang Z, Yu L, Ding M, Tan H, Li J, Fu Q (2011) Polym Chem 2:601–607
4. Auras R, Harte B, Selke S (2004) Macromol Biosci 4:835–864
5. Gupta AP, Kumar V (2007) Eur Polym J 43:4053–4074
6. Dorgan JR, Lehermeier HJ, Palade L-I, Cicero J (2001) Macromol Symp 175:55–66
7. Bai HW, Xiu H, Gao J, Deng H, Zhang Q, Yang MB, Fu Q, Appl ACS (2012) Mater Interfaces 4:897–905
8. Meng B, Tao J, Deng J, Wu Z, Yang M (2011) Mater Lett 65:729–732
9. Theryo G, Jing F, Pitet LM, Hillmyer MA (2010) Macromolecules 43:7394–7397
10. Ljungberg N, Wesslen B (2005) Biomacromolecules 6:1789–1796
11. Oyama HT (2009) Polymer 50:747–751
12. Broz ME, VanderHart DL, Washburn NR (2003) Biomaterials 24:4181–4190
13. Grijpma DW, VanHofslot RDA, Super H, Nijenhuis AJ, Pennings AJ (1994) Polym Eng Sci 34:1674–1684
14. Noda I, Satkowski MM, Dowrey AE, Marcott C (2004) Macromol Biosci 4:269–275
15. Zhang W, Chen L, Zhang Y (2009) Polymer 50:1311–1315
16. Nijenhuis AJ, Colstee E, Grijpma DW, Pennings AJ (1996) Polymer 37:5849–5857
17. Wang RY, Wang SF, Zhang Y, Wan CY, Ma P (2009) Polym Eng Sci 49:26–33
18. Li K, Peng J, Turng LS, Huang HX (2011) Adv Polym Technol 30:150–157
19. Gramlich WM, Robertson ML, Hillmyer MA (2010) Macromolecules 43:2313–2321
20. Robertson ML, Chang K, Gramlich WM, Hillmyer MA (2010) Macromolecules 43:1807–1814
21. Nyambo C, Misra M, Mohanty AK (2012) J Mater Sci 47:5158–5168
22. Takagi Y, Yasuda R, Yamaoka M, Yamane T (2004) J Appl Polym Sci 93:2363–2369
23. Ma P, Hristova-Bogaerds DG, Goossens JGP, Spoelstra AB, Zhang Y, Lemstra PJ (2012) Eur Polym J 48:146–154
24. Li Y, Shimizu H (2009) Eur Polym J 45:738–746
25. Bulota M, Hughes M (2012) J Mater Sci 47:5517–5523
26. Yi-Song H, Jian-Bing Z, Guang-Chen L, Qiu-Tong L, Yu-Zhong W (2014) RSC Adv 4:12857–12866
27. Shuai X, He Y, Asakawa N, Inoue Y (2001) J Appl Polym Sci 81:762–772
28. Qiu JS, Xing CY, Cao XJ, Wang HT, Wang L, Zhao LP, Li YJ (2013) Macromolecules 46:5806–5814
29. Huneault MA, Li HB (2007) Polymer 48:270–280
30. Harada M, Ohya T, Iida K, Hayashi H, Hirano K, Fukuda H (2007) J Appl Polym Sci 106:1813–1820
31. Li YJ, Shimizu H (2007) Macromol Biosci 7:921–928
32. Gurunathan T, Rao CRK, Narayan R, Raju KVSN (2013) J Mater Sci 48:67–80
33. Han JJ, Huang HX (2011) J Appl Polym Sci 120:3217–3223
34. Swamy BKK, Siddaramaiah H, Somashekar R (2003) J Mater Sci 38:451–460
35. Ogunniyi DS (2006) Bioresour Technol 97:1086–1091
36. Gurunathan T, Mohanty S, Nayak SK (2014) J Mater Sci 49:8016–8030
37. Coleman MM, Lee KH, Skrovanek DJ, Painter PC (1986) Macromolecules 19:2149–2157
38. Romanova V, Begishev V, Karmanov V, Kondyurin A, Maitz MF (2002) J Raman Spectrosc 33:769–777
39. Meaurio E, Zuza E, López N, Sarasua JR (2006) J Phys Chem B 110:5790–5800
40. Pan P, Yang J, Shan G, Bao Y, Weng Z, Cao A, Yazawa K, Inoue Y (2012) Macromolecules 45:189–197
41. Lu JM, Qiu ZB, Yang YT (2007) Polymer 48:4196–4204
42. Sakai F, Nishikawa K, Inoue Y, Yazawa K (2009) Macromolecules 42:8335–8342
43. Hong H, Wei J, Yuan Y, Chen FP, Wang J, Qu X, Liu CS (2011) J Appl Polym Sci 121:855–861

44. Jiang L, Wolcott MP, Zhang JW (2006) Biomacromolecules 7:199–207
45. Marubayashi H, Asai S, Sumita M (2012) Macromolecules 45:1384–1397
46. Zhang J, Hu CP (2008) Eur Polym J 44:3708–3714
47. Utracki LA (2003) Polymer blends handbook. Kluwer Academic Publishers, Dordrecht
48. Fenouillot F, Cassagnau P, Majeste JC (2009) Polymer 50:1333–1350
49. Pearson RA, Yee AF (1986) J Mater Sci 21:2462–2474
50. Tseng FP, Lin JJ, Tseng CR, Chang FC (2001) Polymer 42:713–725
51. Chen GX, Kim HS, Kim ES, Yoon JY (2005) Polymer 46:11829–11836
52. Shibata M, Inoue Y, Miyoshi M (2006) Polymer 47:3557–3564
53. Chen R, Zou W, Wu C, Jia S, Huang Z, Zhang G, Yang Z, Qu J (2014) Polym Test 34:1–9
54. Lin Y, Zhang KY, Dong ZM, Dong LS, Li YS (2007) Macromolecules 40:6257–6267
55. Turi EA (1997) Thermal characterization of polymeric materials, 2nd edn. Academic Press, New York, p 793
56. Hashima K, Nishitsuji S, Inoue T (2010) Polymer 51:3934–3939